JOURNAL OF SOLID STATE CHEMISTRY 137, 242–248 (1998)
ARTICLE NO. SC977713

Refinement of the Monoclinic and Tetragonal Structures of Eu^{3+}-Doped $LiYO_2$ by Neutron Diffraction at 77 and 383 K Differential Scanning Calorimetry, and Crystal Field Analysis

M. D. Faucher,* Ph. Sciau,† J-M. Kiat,†,‡ M-G Alves,* and F. Bouree‡

*Laboratoire de Physico-Chimie Moléculaire et Minérale, URA 1907 du CNRS, and †Laboratoire de Chimie Physique du Solide, URA 453 du CNRS, Ecole Centrale de Paris, 92295 Chatenay-Malabry Cedex, France; and ‡Laboratoire Léon Brillouin (CEA-CNRS), Centre d'Etudes de Saclay, 91191 Gif-sur-Yvette Cedex, France

Received April 17, 1997; in revised form October 31, 1997; accepted November 18, 1997

The atomic coordinates and the temperature factors of the β- and α-forms of $LiYO_2$:5% Eu^{3+} at 77 and 383 K, were refined utilizing neutron diffraction data on a powder sample. DSC experiments on an annealed sample show that the monoclinic → tetragonal transition occurs at 69°C during the heating cycle and the reverse at 67°C while cooling. Wide corridors lined by two parallel and adjacent Li–O rows running along the [100] and [010] tetragonal directions allow for the penetration of water, hence the formation of an hydrated crust at the surface of the grains. Theoretical crystal field parameters of Eu^{3+} in C_1 and D_{2d} site symmetries are calculated utilizing the newly refined atomic coordinates. Experimental (empirical) crystal field parameters are fitted utilizing a 387×387 interaction matrix. © 1998 Academic Press

I. INTRODUCTION

A primary interest in the compounds $A^{I}Ln^{III}O_2$ (A^{I} = alkaline metal, Ln^{III} = lanthanide or Y) is due to the bright luminescence of some of these compounds (1–4) under ultraviolet excitation. Not all of these compositions are favorable hosts for efficient phosphors. $NaLuO_2$, which is centro-symmetrical around Lu, is a bad host; $NaGdO_2$, which is strongly distorted, is an excellent one (5). $LiYO_2$ belongs to this second category.

The compounds $LiLnO_2$ have been grouped into four structural forms. The tetragonal α-form (space group: $I4_1/amd$) preferred by small lanthanides (Ln = Lu, Yb, Er) was first described by Hoppe (6) and examined by Bertaut and Gondrand (7). A single-crystal structure refinement of $YbLiO_2$ was recently carried out by Glaum *et al.* (8).

The monoclinic β-form (space group: $P2_1/c$) is adopted by medium sized lanthanide ions (Ln = Y, Ho, Dy). It was discovered by Bertaut and Gondrand (7), who noticed that the diffraction lines of $DyLiO_2$ and $HoLiO_2$ were split into doublets and multiplets, except for the (200) and (004) reflections, which remained single. They pointed out the approximate relations between the cell vectors of the tetragonal α-form and the distorted monoclinic β-form:

$$\mathbf{a}_m = 1/2(\mathbf{a}_t + \mathbf{b}_t + \mathbf{c}_t);\ \mathbf{b}_m = \mathbf{a}_t - \mathbf{b}_t;\ \mathbf{c}_m = 1/2(\mathbf{a}_t + \mathbf{b}_t - \mathbf{c}_t). \quad [1]$$

According to these relations, the monoclinic cell vectors $\mathbf{a}_m$ and $\mathbf{c}_m$ have nearly the same length, and the angle β is nearly equal to 120°. Neutron diffraction was recommended to give the precise positions of the lithium and oxygen ions (7). Reference (9) reports a single crystal study of β–$LiYO_2$ by Stewner and Hoppe.

Two other forms have been found. The γ-form (orthorhombic, space group: *Pbnm*; Ln = Tb, Gd, Eu, Sm was found simultaneously by Gondrand and Bertaut (10) and Bärnighausen (11), then examined again in Ref. (12). The structure of γ-$TbLiO_2$ was solved by Gondrand (13). The other structure is the δ-form (monoclinic; space group: $P2_1/c$; Ln = Eu, Sm, Nd, Pr, La) (14–16). The nomenclature of the different forms was clarified in Ref. (17). Lithium yttriate preferably adopts the α- and β-forms.

The physical properties of the $A^{I}M^{III}O_2$ compounds with A = Li–Cs have been extensively investigated during the past 30 years (18). These "simple" structures display a series of contradictory features. The tetragonal variety referred to as the α-$LiFeO_2$ type structure has been defined as a "stuffed" derivative of the anatase type rather than an ordered variety of the NaCl type (19). What is intriguing, for instance, is the high c/a ratio, which may attain 2.3. There is no close packing of spheres. The Madelung constant or the Madelung part of the lattice energy is nearly the same whether an ideal arrangement of the ligands (ligands equidistant to the metals) or the true experimental arrangement is considered. The coordination polyhedron around Li is almost planar (19).

0022-4596/98 $25.00

At room temperature, pure $LiYO_2$ exists in the β-form. Rare earth-doped compounds $LiYO_2$:5% Ln^{3+} are monoclinic $P2_1/c$ (the β-form) at room temperature for $Ln =$ Pr–Tm and tetragonal $I4_1/amd$ (the α-form) for $Ln =$ Yb and Lu (4). The structure depends on the mean rare earth radius, and the critical ionic radius for which the structure switches from one form to the other is 0.899 Å. Pure $LiYO_2$ inserts itself between $LiYO_2$:5% Eu^{3+} and $LiYO_2$:5% Tb^{3+} (Table 1 in Ref. (4)).

Upon heating to 350 K, monoclinic $LiYO_2$:5% Eu^{3+} transforms into the tetragonal α-form (20). Fluorescence measurements of the compound were previously performed at 77, 300, and 370 K (20). Given the extreme sensitivity of the structure to temperature, precise atomic coordinates are needed under conditions close to those of the optical investigations if some correlation between structure and spectra is to be attempted.

The coordinates and overall temperature factors of the tetragonal form were obtained previously by X-ray diffraction experiments (4). It was, however, impossible to obtain precise values for the anisotropic temperature factors of this form and for the 12 atomic coordinates of the monoclinic form. We now rely on a neutron diffraction experiment to provide the missing data for the β (low temperature) and α (high temperature) forms of $LiYO_2$:5% Eu^{3+}.

II. SYNTHESIS—DIFFERENTIAL SCANNING CALORIMETRY—THERMAL DECOMPOSITION

The $LiY_{0.95}Eu_{0.05}O_2$ powder sample was prepared by precipitating a mixed ($Ln = Y + Eu$) rare earth chloride solution with oxalic oxide. The precipitate was washed, dried, and fired in an alumina crucible with an excess of lithium carbonate at 980°C for 2 h and then cooled to room temperature in 2 h (4). It was noticed that if the cooling were too slow or the temperature held at 500°C, the lithiate would decompose into the oxides. What happens is that at high temperature, the rate of decomposition of the carbonate and its reaction with the activated oxides produced by the oxalate decomposition is faster than the decomposition rate of $LiYO_2$, whereas during cooling the carbonate no longer decomposes, no fresh lithiate is produced, but the decomposition of $LiYO_2$ proceeds. Thus, although stable at room temperature, the α-form of $LiYO_2$:5% Eu^{3+} undergoes a steady decomposition process into the oxides, starting at about 250°C. This represents a serious drawback to its utilization in phosphors.

After a quantitative analysis of yttrium, europium, lithium, and carbone, our powder sample contained 0.5% unreacted Li_2CO_3 (molar) and 0.95% $LiY_{0.95}Eu_{0.05}O_2$.

A weak hygroscopic behavior of $LiYO_2$ was pointed out by Rozdin *et al.* (21). Accordingly, an investigation of the thermal behavior of the sample was undertaken prior to the neutron experiment by differential scanning calorimetry (DSC)—complementing anterior DTA analyses (22)—and X-ray diffraction. The first DSC run on a newly prepared sample (using a Seiko SC220C) from room temperature to 300°C at a 5°/min. heating rate displays an endothermic peak at 73°C corresponding to the monoclinic → tetragonal transition and several weak, diffuse exothermic peaks between 190 and 250°C (Fig. 1, cycle 1). This second group is assigned to the departure of water. After the first heating, some oxide Y_2O_3 is detected in the diffraction pattern. In the course of a second heating the transition peak appears alone at 69°C (Fig. 1, cycle 2). The transition temperature does not change any more if other heating cycles are done. The monoclinic → tetragonal transition occurs 4° higher in the hydrated sample than in the thermally "dried" sample. When cooling to room temperature, the sharp peak indicating the reverse phase transition from the tetragonal to the monoclinic form occurs at 67°C.

The same experiment repeated after exposure to air in normal conditions for some days displays, again, the group of peaks between 190 and 250°C.

X-ray diagrams were recorded during the heating and cooling periods. The powder was lightly pressed and maintained in the sample holder by a beryllium window. The temperature was raised to 250°C by steps, held constant for 3 h, and then cooled.

Attention was paid to the line shapes and positions in the tetragonal form during the heating and cooling periods. At 90°C, first step of the heating period, lines *001* are broader than *h00* or *hk0*. From 90 to 190°C there is no visible evolution other than thermal expansion. At 200 and 250°C the *001* lines sharpen quickly. On cooling to 90°C, they retain their sharpness and are significantly displaced with respect to their initial positions. A refinement of the tetragonal cell parameters for the (90H) (heating) and (90C) (cooling)

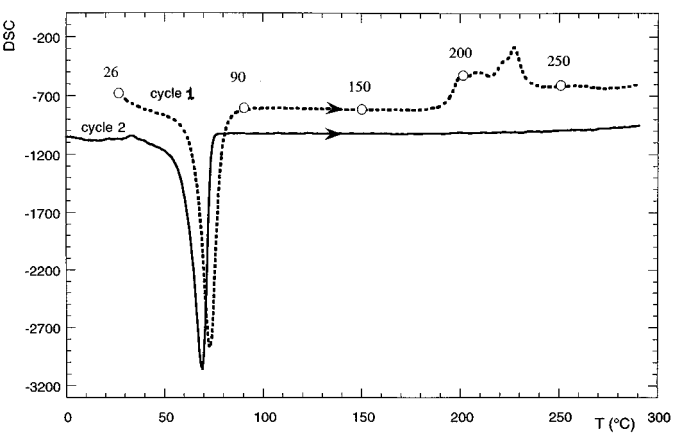

FIG. 1. Two DSC runs of the $LiYO_2$:Eu^{3+} sample. In a parallel experience, X-ray diffraction was performed at the temperatures indicated on the curve. At the second heating, the transition peak is 4° lower and the spurious peaks have disappeared.

spectra gives the following values:

Parameters (Å)	90H	90C
a_t	4.444(3)	4.447(3)
c_t	10.390(6)	10.372(6)

The c_t parameter has slightly decreased, while the a_t parameter has very slightly increased.

The intensity of the strongest *222* line of the oxide Y_2O_3 was recorded at each step (Fig. 2). It appears at 200°C, increases rapidly at 250°C, and swells steadily when the heating period is prolonged for 3 h.

The sharpening of the diffraction lines of $LiYO_2$ and the decomposition of the sample into the oxides on heating are obviously closely connected. This will be further discussed in Section III but we note here that a correct structural analysis on a "stabilized" sample requires a short annealing period at 250°C.

III. STRUCTURE REFINEMENT

The experiments were run on a thermally "stabilized" powder sample on the 3T2 high resolution powder diffraction device at Laboratoire Léon Brillouin using the Orphée reactor facilities. The two-axis diffractometer is installed on a canal of thermal neutrons impinging on a germanium monochromator ($\lambda = 1.2272$ Å). The sample is located in a cryofurnace, allowing operations from 1.5 to 600 K. The data were refined by program XND designed by Bérar (23). Excess nonreacted lithium carbonate was taken into account as a second phase in the refinement process. The cell parameters and refined atomic positions of the monoclinic and tetragonal forms are reported in Tables 1 and 2. Anisotropic B factors were refined for yttrium and oxygen in the quadratic form at 110°C. An isotropic B factor was refined for Li in the two structures and for all the atoms in the monoclinic form. The occupation factor of Li in the tetragonal form was found equal to 0.13, slightly in excess (4%) to the theoretical value (0.125).

The final reliability factors R_B and R_{wp} are equal to 0.044 and 0.059 respectively for the monoclinic phase, 0.035 and 0.058 respectively for the tetragonal phase.

The projection on the (001) tetragonal plane is represented in Figs. 3a and 3b. The monoclinic form is rotated to facilitate a comparison between the structures. The successive rotations that allow the monoclinic cell to be viewed along the pseudotetragonal c-axis are : 31.3, 90, and 143° around b_m, u_m ($\perp$ to c_m in the c_m, a_m plane), and b_m (old axes) respectively. Figures 4a and 4b represent a projection of both structures on a (010) tetragonal plane.

In Figs. 3 and 4, the thermal vibration ellipses are represented according to the values given in Tables 1 and 2. It can be stated that in the tetragonal structure, yttrium and oxygen vibrate weakly along the four horizontal Y–O bonds, but much more along c_t. In both structures, there are wide corridors made of two parallel and adjacent Li–O rows along the [100] direction (Fig. 4b). Within the area limited by these two rows, the lithium and oxygen atoms vibrate strongly along [100] and [001] as well (Fig. 4b). Similar rows occur in the perpendicular [010] direction. It is not understood why these corridors are so wide (the mean vertical Li–O distance is 3.06 Å).

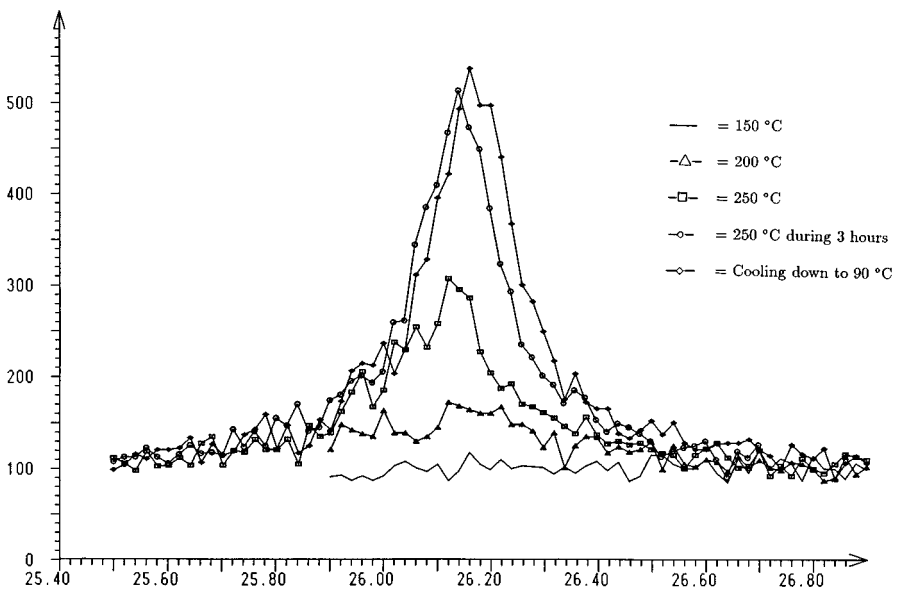

FIG. 2. Intensity of the *222* diffraction line of the oxide Y_2O_3 recorded at each heating step and back down to 90°C.

TABLE 1

Cell Parameters (Å), Refined Atomic Positions, Volume (Å^3), and Overall Temperature Factors (Å^2) in Monoclinic $LiYO_2$: 5% Eu^{3+} at 77 K

	$LiYO_2:Eu^{3+}$ (77 K)	Monoclinic $P2_1/c$
	a_m	6.1493(8)
	b_m	6.1500(10)
	c_m	6.2494(2)
	β_m	119.091(5)
	Volume	206.53
Yttrium	x	0.2340(4)
(4e)	y	0.1312(4)
	z	−0.0207(4)
	B	0.21(3)
Lithium	x	0.291(2)
(4e)	y	0.654(1)
	z	0.068(1)
	B	0.6(1)
Oxygen 1	x	0.4541(5)
(4e)	y	0.3930(5)
	z	0.2622(5)
	B	0.28(5)
Oxygen 2	x	−0.0121(5)
(4e)	y	0.1712(4)
	z	0.1561(5)
	B	0.29(5)
	R_B	0.0440
	R_{wp}	0.0594
	R_{exp}	0.051

Note. Standard deviations are in parentheses.

TABLE 2

Cell Parameters (Å), Refined Atomic Positions, Volume (Å^3), Anisotropic Temperature Factors, Global Temperature Factors (Å^2), and T Occupation Factor of Lithium in Tetragonal $LiYO_2$:5% Eu^{3+} at 383 K

	$LiYO_2:Eu^{3+}$ (370 K)	Tetragonal $I4_1/amd$
	a_t	4.4468(9)
	c_t	10.372(2)
	Volume	205.10
Yttrium	$x = y = z$	0
(4a)	$B11 = B22$	0.0095(4)
	$B33$	0.0004(1)
	T	0.130(2)
Lithium	$x = y$	0
(4b)	z	0.5
	B	2.5(2)
Oxygen	$x = y$	0
(8e)	z	0.2230(1)
	$B11$	0.0270(7)
	$B22$	0.0041(6)
	$B33$	0.0038(2)
	R_B	0.035
	R_{wp}	0.0575
	R_{exp}	0.051

Note. Standard deviations are in parentheses.

The coordination polyhedra around lithium are quite unusual. In $LiNbO_3$ (24), for instance, the coordination polyhedron is a distorted octahedron with mean Li–O distance equal to 2 Å. In the tetragonal form of $LiYO_2$, the coordination polyhedron of Li is almost planar with four short Li–O distances (2.24 Å) in the (001) plane and two longer Li–O distances (2.87 Å) perpendicular to it. In the monoclinic form, the coordination polyhedron is also quasi-planar but triangular. There are three short Li–O distances ($\approx$2 Å) in the (001) plane and three longer distances (average value = 3.06 Å), one in the (001) plane and two perpendicular to it (Table 3).

The hydratation process can now be better understood. Hydrogen may be able to diffuse along the wide corridors. If we consider the geometry of LiOH, the distances Li–O = 1.96 Å and O–H = 0.92 Å. The non bonding Li–H distance = 2.50 Å, while the Li–O–H angle is close to 120° (25). Therefore one can imagine a local distortion in $LiYO_2$ in which the horizontal Li–O distance is decreased to below 2 Å and the vertical Li–O distance is increased to allow the insertion of hydrogen between Li and H on a vertical row. This hypothesis is consistent with the larger c_t (respectively smaller a_t) parameter before the heat treatment. The contamination of the sample would affect the areas close to the surface of the grains. The heat treatment would destroy the hydrogen bonds and lead to the decomposition of the "contaminated" part of the sample. But this explains only a small part of the problem, and does not address the very large vertical Li–O distances that remain after the heat treatment.

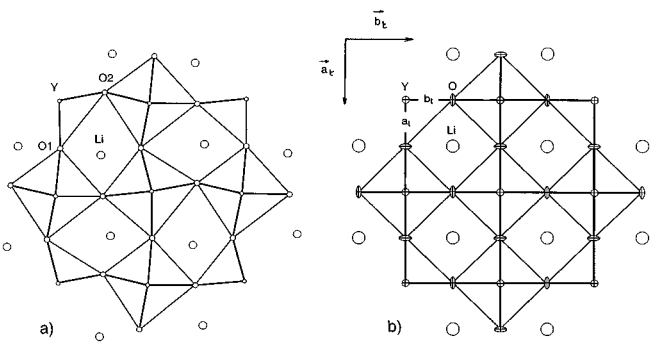

FIG. 3. Projection of the monoclinic and tetragonal structures of $LiYO_2:Eu^{3+}$ on the (001) tetragonal plane. The monoclinic structure has been rotated to show in an unambiguous way the similar deformation of the two coordination polyhedra with respect to the regular octahedral symmetry.

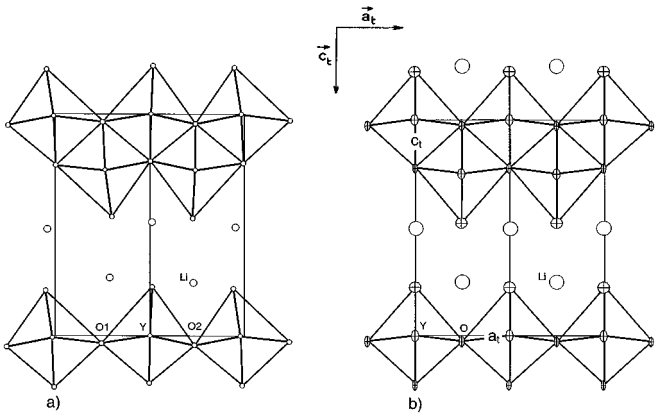

FIG. 4. Projection of the monoclinic and tetragonal structures of $LiYO_2:Eu^{3+}$ on the (010) tetragonal plane.

IV. CRYSTAL FIELD PARAMETERS

Spectroscopic studies on europium doped $LiYO_2$ were performed earlier and sets of experimental crystal field parameters were determined (4, 20). A new refinement was carried out with reference to the experimental $4f^6$ energy levels measured at 77 and 370 K reported in Table 6 of Ref. (4). Instead of a 49×49 (^{7}F) basis set, we utilized program *fn* (26), which works on a larger matrix, *i.e.*, a 387×387 basis set. It was shown that this set is large enough to provide a satisfactory representation of the ^{7}F manifold energy level scheme (27).

In the tetragonal form, Li, Y, and the substituted europium have the site symmetry $\bar{4}m2$ (D_{2d}) while in the monoclinic form, all ions are in general positions (C_1). In both forms, the oxygen ligands form a distorted octahedron. The newly refined crystal structures were utilized to estimate theoretical values of the crystal field parameters. The monoclinic cell was rotated to orient the O_z axis for the calculation along the pseudotetragonal axis. In the C_1 symmetry, all 27 (ff) crystal field parameters are allowed. A "covalo-electrostatic" evaluation [28–30] was used to select the largest parameters. All parameters calculated are listed in the first column of Table 4. It should be stressed that the predicted B_0^2 parameter given in Ref. (4), Table 8 for the tetragonal form is erroneous. The electrostatic part should be $-378\,cm^{-1}$ and the total B_0^2 (listed in column *C–E*) should be equal to $-605\,cm^{-1}$, which is quite close to the present value. This is not surprising since the unique adjustable parameter of the tetragonal structure was already well determined in (4).

The "covalo-electrostatic" values of the crystal field parameters were utilized as a starting set for the crystal field refinement. Not all the possible 27 B_q^k were retained but only those with $k = 2$, and those larger than $100\,cm^{-1}$ for $k = 4$ and 6 . Among the free-ion parameters, only E_0 and the spin-orbit coupling constant ζ were varied. E_1, E_2, and E_3 were ascribed values previously determined in oxychlorides (31). For the monoclinic phase, S_2^2, B_1^2, and B_3^4 fell to zero during the refinement, and a nonzero S_4^6 improved the agreement. The 10 parameters B_0^2, S_1^2, B_2^2, B_0^4, B_1^4, S_1^4, B_4^4, B_0^6, B_4^6, and S_4^6 were therefore utilized. For the tetragonal phase, the five relevant crystal field parameters in D_{2d} are B_0^2, B_0^4, B_4^4, B_0^6, and B_4^6. The final values of the parameters in both forms are reported in Table 4 together with the electrostatic and covalent contributions of the "predicted" values. In the last column, the tetragonal parameters calculated from the structural data in Ref. (9) are listed. The deviations and RMS values are listed as well. The results are not very different from previously published values obtained in a 49×49 interaction matrix (4). However, the deviations are larger than those reported in Ref. (4), in which experimental and calculated crystal field splitted components were barycentered within each level. The fluorescence lines are broader in the high temperature phase, a fact that can partly explain the larger RMS of the fit.

TABLE 3
Y–O and Li–O Distances and O–Y–O and O–Li–O Angles in YO_6 and LiO_6 Octahedra

Distances (Å)

Monoclinic		Tetragonal	
At1–At2	*R*	At1–At2	*R*
Y–O1	2.285(4)	Y–O	2.241(3) (×4)
Y–O2	2.217(4)	Y–O	
Y–O1	2.328(4)	Y–O	
Y–O2	2.208(4)	Y–O	
Y–O2	2.280(3)	Y–O	2.313(3) (×2)
Y–O1	2.341(3)	Y–O	
Li–O1	2.03(1)	Li–O	2.24(1) (×4)
Li–O2	3.07(1)	Li–O	
Li–O1	1.97(1)	Li–O	
Li–O2	1.93(1)	Li–O	
Li–O2	2.97(1)	Li–O	2.87(1) (×2)
Li–O1	3.15(1)	Li–O	

Angles

Monoclinic		Tetragonal	
Atoms	Angle	Atoms	Angle
O1–Y–O2	155.4°(2)	O–Y–O	165.6°(2) (×2)
O1–Y–O2	161.4°(2)	O–Y–O	
O1–Y–O2	174.2°(2)	O–Y–O	180.0°
O1–Li–O2	155.3°(7)	O–Li–O	165.6°(2) (×2)
O1–Li–O2	155.4°(4)	O–Li–O	
O1–Li–O2	174.5°(4)	O–Li–O	180.0°

Note. Standard deviations are in parentheses.

TABLE 4
Experimentally Fitted Crystal Field Parameters at 77 and 370 K

	Symmetry C_1 ($P2_1/c$) Temperature 77 K		D_{2d} ($I4_1/amd$) 370 K		D_{2d} Ref. (9)
Parameters	Experiment (cm^{-1})	(C–E) (cm^{-1})	Experiment (cm^{-1})	(C–E) (cm^{-1})	(C–E) (cm^{-1})
B_0^2	− 255	− 366 (− 236 − 130)	− 629	− 623 (− 402 − 221)	513
B_1^2	0	− 33 (− 21 − 12)			
S_1^2	− 230	− 43 (− 28 − 15)			
B_2^2	− 89	− 31 (− 20 − 11)			
S_2^2	0	− 45 (− 29 − 16)			
B_0^4	2378	1937 (500 + 1437)	2892	2205 (568 + 1637)	2652
B_1^4	− 38	− 206 (− 53 − 153)			
S_1^4	− 385	− 365 (− 95 − 271)			
B_3^4	0	105 (34 + 71)			
B_4^4	1573	1404 (337 + 1067)	2036	1637 (383 + 1254)	1497
B_0^6	670	495	293	351	1071
B_4^6	− 649	− 476	− 905	− 698	− 519
S_4^6	462	0			
δ^a	11.8		18.3		
RMS[b]	13.9		20.4		
Levels	43		36		

Note. Predicted crystal field parameters are calculated by the covalo-electrostatic model for Eu^{3+} in the monoclinic and tetragonal phases (C–E). Electrostatic and covalent contributions to the *cfp* are in parantheses.

[a] $\delta = (\sum_{i=1,n}(Ei_{exp} - Ei_{calc})^2/n)^{1/2}$, where n = number of levels.

[b] $\mathrm{RMS} = (\sum_{i=1,n}(Ei_{exp} - Ei_{calc})^2/(n - n_p))^{1/2}$, where n_p = number of parameters.

A positive point to note is that the estimated B_0^2 of Eu^{3+} in the tetragonal form ($-623\ cm^{-1}$) is much closer to the experimental value ($-629\ cm^{-1}$) than that calculated from the atomic positions given in Ref. (9) ($+513\ cm^{-1}$). However, the calculation is unable to predict the large parameters with a precision better than 20%, whereas the prediction of small parameters is anarchic. In addition, the variation of the predicted $k = 4$ parameters due to modifications of the atomic positions at the monoclinic → tetragonal phase transition is unable to account for the strong increase of the crystal field parameters in the tetragonal form.

V. CONCLUSION

The crystal structure of $LiYO_2$ doped with 5% europium in powder form was refined at 77 and 383 K (110°C) utilizing neutron diffraction. Low reliability factors were obtained on a freshly annealed powder batch in which the superficial hydrated crust had been decomposed. DSC measurements indicate that the transition temperature from the monoclinic → tetragonal form of the hydrated sample is 73°C, which confirms the earlier measured value (20). The true transition temperature of the annealed sample is 69°C. The cell parameters and atomic positions of the monoclinic and tetragonal forms were refined, as were anisotropic *B* factors for yttrium and oxygen in the quadratic form at 110°C.

In the structure, there are wide corridors made of two adjacent Li–O rows along the [100] and [010] directions. The hydratation process can therefore be explained as the diffusion of hydrogen a limited distance along these corridors. The decomposition of the compound through heating is therefore explained as a result of the destruction of the hydrogen bonds, which causes the contaminated zone to decompose into the oxides rather than reversing into the lithiate.

Kuo *et al.* (19) already pointed out the nearly planar coordination of Li in the tetragonal form of $LiYO_2$, due to four short Li–O distances in the (001) plane. The present work shows that in the monoclinic form, the coordination polyhedron of Li is also quasi-planar but triangular, with three short Li–O distances in the (001) plane.

A crystal field analysis of Eu^{3+} in $LiYO_2$ was carried out in a 387×387 interaction matrix utilizing Eu^{3+} energy levels measured earlier at 77 and 370 K. The refined atomic parameters were utilized to estimate starting theoretical values of the crystal field parameters. Only 10 of the 27 possible crystal field parameters in a C_1 symmetry were retained as a result of the preliminary theoretical estimation. At the transition temperature, the increase of the predicted

$k = 4$ crystal field parameters is equal to 16%, whereas the increase of the experimental (fitted) parameters is equal to 28%.

With the exception of the imaginary component S_4^6, no crystal field parameter other than those predicted by theory seems useful to improve the experimental/calculated fit of the monoclinic form.

ACKNOWLEDGMENT

The authors wish to thank Messieurs Jacques Chevrevil and Gilles Boëmare for their help in X-ray and DSC experiments.

REFERENCES

1. G. Blasse and A. Bril, *J. Chem. Phys.* **45,** 3327 (1966).
2. L. H. Brixner, *J. Electrochem. Soc. Solid State Science* **114,** 252 (1967).
3. P. M. Jaffe and J. D. Konitzer, *J. Electrochem. Soc.* **116,** 633 (1969).
4. M. D. Faucher, O. K. Moune, M-G Alves, B. Piriou, Ph. Sciau, and M. Pham-Thi, *J. Solid State Chem.* **121,** 457 (1996).
5. G. Blasse and B. C. Grabmaier, "Luminescent Materials," p. 44. Springer-Verlag, Berlin-NewYork, (1994).
6. R. Hoppe, *Angew. Chem.* **71,** 457 (1959).
7. F. Bertaut and M. Gondrand, *C. R. Acad. Sci.* **255,** 1135 (1962).
8. H. Glaum, S. Voigt, and R. Hoppe, *Z. Anorg. Allg. Chem.* **598/599,** 129 (1991).
9. F. Stewner and R. Hoppe, *Z. Anorg. Allg. Chem.* **380,** 250 (1971).
10. M. Gondrand and F. Bertaut, *Bull. Soc. Franc. Minér. Crist.* **86,** 301 (1963).
11. H. Bärnighausen, *Acta Crystallogr.* **16,** 1073 (1963).
12. N. I. Sevost'yanova, I. A. Murav'eva, L. M. Kovba, L. I. Martynenko, and V. I. Spitsyn, *Dokl. Akad. Nauk SSSR* **161,** 1359 (1965).
13. M. Gondrand, *Bull. Soc. Franc. Minér. Crist.* **96,** 166 (1973).
14. H. Bärnighausen, *Acta Crystallogr.* **19,** 1048 (1965).
15. M. Gondrand, *Bull. Soc. Franc. Minér. Crist.* **90,** 107 (1967).
16. M. Gondrand, *Bull. Soc. Franc. Minér. Crist.* **93,** 421 (1970).
17. M. Waintal and M. Gondrand, *Mater. Res. Bull.* **2,** 889 (1967).
18. R. Hoppe and H. Sabrowsky, *Z. Anorg. Allg. Chem.* **357,** 202 (1968).
19. Y. B. Kuo, W. Scheld, and R. Hoppe, *Z. Kristallogr.* **164,** 121 (1983).
20. M. Faucher, O. K. Moune, L. Albert, and B. Piriou, *C.R. Acad. Sci. Paris II* **317,** 1569 (1993).
21. I. A. Rozdin, H. T. Saripov, S. S. Plotkin, N. V. Brotnikov, T. B. Polueva, and K. I. Petrov, *Izv. Akad. Nauk SSSR Neorg. Mater.* **12,** 863 (1976).
22. J. Hölsa, M. Faucher, J.-M. Kiat, M. Lastusaari, and E. Saïlynoja, "DTA study of the monoclinic to tetragonal phase transformation in RE^{3+} doped $LiYO_2$." 15th Nordic Symposium for Thermal Analysis and Calorimetry, Helsinki, 13–15 November, 1996.
23. J. F. Bérar and P. Garnier, APD 2nd Conference. N.I.S.T. (U.S.) Gaithersburg, May, 1992.
24. R. W. G. Wyckoff, "Crystal Structures," Vol. 2, p. 420. Interscience Publishers, New York, 1964.
25. R. W. G. Wyckoff, "Crystal Structures," Vol. 1, p.136. Interscience Publishers, New York, 1963.
26. M. Faucher, unpublished program.
27. O. K. Moune and P. Caro, *J. Less Common Metals* **148,** 181 (1989).
28. M. Faucher, Program CHLOE, *in* "Logiciels pour la Chimie," p. 60. ANL-SFC, 1991.
29. D. Garcia and M. Faucher, *J. Chem. Phys.* **82,** 5554 (1985).
30. M. Faucher, D. Garcia, and O. K. Moune, *J. Lumin.* **51,** 341 (1992).
31. J. Hölsa and P. Porcher, *J. Chem. Phys.* **75,** 2108 (1981).